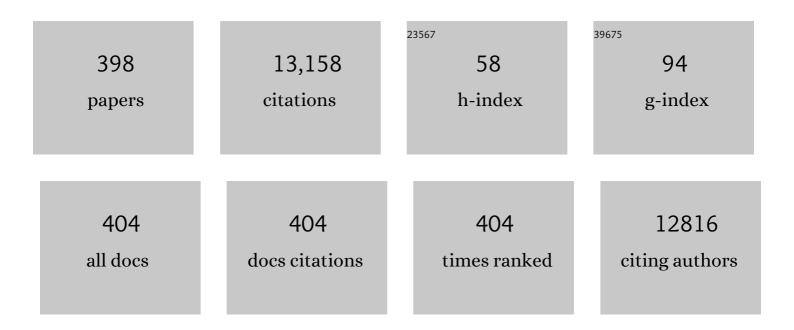
## Ashok Kumar

List of Publications by Year in descending order

Source: https://exaly.com/author-pdf/351910/publications.pdf Version: 2024-02-01



| #  | Article   | IF  | CITATIONS |
|----|---|-----|-----------|
| 1  | Optimal vitamin D level ameliorates neurological outcome and quality of life after traumatic brain injury: a clinical perspective. International Journal of Neuroscience, 2023, 133, 417-425.   | 1.6 | 2         |
| 2  | Emergency Department Management of Mild Traumatic Brain Injury in New Delhi–A Single Institute<br>Cohort Management Data. Indian Journal of Neurosurgery, 2022, 11, 123-127.  | 0.2 | 2         |
| 3  | Facile wet chemical synthesis and electrochemical performance of double perovskite- La2NiMnO6 for energy storage application. Materials Today: Proceedings, 2022, 48, 587-589.  | 1.8 | 4         |
| 4  | Effects of Sm3+ ions on the structural, optical and thermoluminescence properties of MnKB glass system. Journal of Physics and Chemistry of Solids, 2022, 161, 110408.  | 4.0 | 4         |
| 5  | Evaluating potential of tissueâ€engineered cryogels and chondrocyte derived exosomes in articular cartilage repair. Biotechnology and Bioengineering, 2022, 119, 605-625.   | 3.3 | 25        |
| 6  | Understanding the control of inclusion of SrO to the Li2O -K2O-B2O3-SrO glasses on the physical,<br>structural, and gamma ray shielding performance. Journal of the Australian Ceramic Society, 2022, 58,<br>205-216.                                 | 1.9 | 2         |
| 7  | Fire incidents in Bed-head panels: Causes and recommendations for prevention. Journal of Family<br>Medicine and Primary Care, 2022, 11, 360.  | 0.9 | Ο         |
| 8  | Robot-assisted and conventional urology surgical procedures: comparison of average length of stay,<br>economic status, operative time and patient's expenditure in a tertiary care hospital of North India.<br>Journal of Robotic Surgery, 2022, , 1. | 1.8 | 1         |
| 9  | Responsive polymerâ€assisted 3D cryogel supports Huh7.5 as in vitro hepatitis C virus model and ectopic<br>human hepatic tissue in athymic mice. Biotechnology and Bioengineering, 2021, 118, 1286-1304.  | 3.3 | 2         |
| 10 | Angst, panic and stigma concomitant to COVID-19 deceased. Asian Journal of Psychiatry, 2021, 55, 102527.  | 2.0 | 1         |
| 11 | A broadband circularly polarized monopole antenna for millimeterâ€wave short range 5G wireless<br>communication. International Journal of RF and Microwave Computer-Aided Engineering, 2021, 31,<br>e22518.   | 1.2 | 13        |
| 12 | Recent Advances in Biomaterialâ€Based Highâ€Throughput Platforms. Biotechnology Journal, 2021, 16,<br>2000288.  | 3.5 | 5         |
| 13 | Alternate pathway for standard SCR on Cu-zeolites with gas-phase ammonia. Reaction Chemistry and Engineering, 2021, 6, 1042-1052.   | 3.7 | 17        |
| 14 | Rare-earth (Dy)-doped (GeS2)80(In2S3)20 thin film: influence of annealing temperature in argon<br>environment on the linear and nonlinear optical parameters. Applied Physics A: Materials Science and<br>Processing, 2021, 127, 1.                   | 2.3 | 9         |
| 15 | Alkaline Earth Stannate Nanomaterials as an Electron Transport Layer in Dye-Sensitized Solar Cells. ,<br>2021, , 1-22.  |     | Ο         |
| 16 | Tailoring Dy3+/Tb3+-doped lead telluride borate glasses for gamma-ray shielding applications.<br>European Physical Journal Plus, 2021, 136, 1.  | 2.6 | 5         |
| 17 | Multidimensional dynamic healthcare personnel (HCP)-centric model from a low-income and<br>middle-income country to support and protect COVID-19 warriors: a large prospective cohort study.<br>BMJ Open, 2021, 11, e043837.                          | 1.9 | 7         |
| 18 | rGO/PEDOT:PSS/NiMn <sub>2</sub> O <sub>4</sub> Nanohybrid: An Inexpensive Anode Catalyst for<br>Methanol and Ethylene Glycol Electro-Oxidation. Journal of the Electrochemical Society, 2021, 168,<br>034510.   | 2.9 | 4         |

Ashok Kumar

| #  | Article  | IF  | CITATIONS |
|----|--|-----|-----------|
| 19 | X- ray absorption parameters studies of P2O5- SnCl2-SnO bioactive glass system. Journal of X-Ray<br>Science and Technology, 2021, 29, 373-382.   | 1.0 | 0         |
| 20 | Optical, mechanical properties and gamma ray shielding behavior of TeO2-Bi2O3-PbO-MgO-B2O3 glasses using FLUKA simulation code. Optical Materials, 2021, 113, 110900.  | 3.6 | 47        |
| 21 | Fabrication of TeO2-doped strontium borate glasses possessing optimum physical, structural, optical and gamma ray shielding properties. European Physical Journal Plus, 2021, 136, 1.  | 2.6 | 8         |
| 22 | A comprehensive investigation on the role of PbO in the structural and radiation shielding attribute<br>of P2O5–CaO–Na2O–K2O–PbO glass system. Journal of Materials Science: Materials in Electronics,<br>2021, 32, 12371-12382. | 2.2 | 14        |
| 23 | Understanding the role of Bi2O3 in the P2O5–CaO–Na2O–K2O glass system in terms of physical,<br>structural and radiation shielding properties. Journal of Materials Science: Materials in Electronics,<br>2021, 32, 11649-11665.  | 2.2 | 16        |
| 24 | Exosome-Functionalized Ceramic Bone Substitute Promotes Critical-Sized Bone Defect Repair in Rats.<br>ACS Applied Bio Materials, 2021, 4, 3716-3726.   | 4.6 | 16        |
| 25 | Physical, structural, and gamma ray shielding studies on novel (35+x) PbO-5TeO2-20Bi2O3-(20-x)<br>MgO-20B2O3 glasses. Journal of the Australian Ceramic Society, 2021, 57, 971-981.  | 1.9 | 7         |
| 26 | In-depth survey of nuclear radiation attenuation efficacies for high density bismuth lead borate glass system. Results in Physics, 2021, 23, 104030.   | 4.1 | 27        |
| 27 | Detailed Inspection of γ-ray, Fast and Thermal Neutrons Shielding Competence of Calcium Oxide or<br>Strontium Oxide Comprising Bismuth Borate Glasses. Materials, 2021, 14, 2265.  | 2.9 | 33        |
| 28 | Tailoring bismuth borate glasses by incorporating PbO/GeO2 for protection against nuclear radiation.<br>Scientific Reports, 2021, 11, 7784.  | 3.3 | 22        |
| 29 | Thermoluminescence, structural and optical properties of Ce3+ doped borosilicate doped glasses.<br>Journal of Materials Science: Materials in Electronics, 2021, 32, 18381-18396.  | 2.2 | 21        |
| 30 | Probing of nuclear radiation attenuation and mechanical features for lithium bismuth borate glasses with improving Bi2O3 content for B2O3Â+ÂLi2O amounts. Results in Physics, 2021, 25, 104246.                                  | 4.1 | 30        |
| 31 | Mechanical and Gamma-Ray Interaction Studies of PbO–MoO3–Li2O–B2O3 Glass System for Shielding<br>Applications in The Low Energy Region: A Theoretical Approach. Applied Sciences (Switzerland), 2021, 11,<br>5538.               | 2.5 | 1         |
| 32 | Mapping B-Cell Epitopes for Nonspecific Lipid Transfer Proteins of Legumes Consumed in India and<br>Identification of Critical Residues Responsible for IgE Binding. Foods, 2021, 10, 1269.                                      | 4.3 | 3         |
| 33 | Effect of Add-On Therapy of Sodium-Glucose Cotransporter 2 Inhibitors and Dipeptidyl Peptidase 4<br>Inhibitors on Adipokines in Type 2 Diabetes Mellitus. Journal of Clinical Medicine Research, 2021, 13,<br>355-362.           | 1.2 | 2         |
| 34 | Miniaturized High-Power Beam Steering Network Using Novel Nonplanar Waveguide Butler Matrix.<br>IEEE Microwave and Wireless Components Letters, 2021, 31, 678-681.   | 3.2 | 4         |
| 35 | Mechanical and Gamma Ray Absorption Behavior of PbO-WO3-Na2O-MgO-B2O3 Glasses in the Low<br>Energy Range. Materials, 2021, 14, 3466.   | 2.9 | 16        |
| 36 | Spinal cord regeneration: A brief overview of the present scenario and a sneak peek into the future.<br>Biotechnology Journal, 2021, 16, e2100167.   | 3.5 | 7         |

| #  | Article  | IF   | CITATIONS |
|----|--|------|-----------|
| 37 | Physical, optical, structural and thermoluminescence behaviour of borosilicate glasses doped with trivalent neodymium ions. Optical Materials, 2021, 117, 111109.  | 3.6  | 20        |
| 38 | Periosteum-Mimicking Tissue-Engineered Composite for Treating Periosteum Damage in Critical-Sized<br>Bone Defects. Biomacromolecules, 2021, 22, 3237-3250.   | 5.4  | 23        |
| 39 | Experimental and Theoretical Study of Radiation Shielding Features of CaO-K2O-Na2O-P2O5 Glass<br>Systems. Materials, 2021, 14, 3772.   | 2.9  | 59        |
| 40 | Prevalence of 25-Hydroxyvitamin D Deficiency and its severity correlation with Acute Traumatic brain<br>Injury in Indian Patients: A Perspective Observation Study. Research Journal of Pharmacy and<br>Technology, 2021, , 3874-3878. | 0.8  | 3         |
| 41 | Electronic and optical properties of boron-based hybrid monolayers. Nanotechnology, 2021, 32, 415203.  | 2.6  | 2         |
| 42 | An RNAi-independent role of AP1-like stress response factor Pap1 in centromere and mating-type silencing in Schizosaccaromyces pombe. Journal of Biosciences, 2021, 46, 1.   | 1.1  | 2         |
| 43 | Synthesis, structural investigation, mechanical calculations and photon shielding properties of<br>CaO–K2O–Na2O–P2O5 glass system. Optical Materials, 2021, 117, 111178.   | 3.6  | 9         |
| 44 | Ferrite application as an electrochemical sensor: A review. Materials Characterization, 2021, 178, 111269.   | 4.4  | 54        |
| 45 | Transplantation of engineered exosomes derived from bone marrow mesenchymal stromal cells<br>ameliorate diabetic peripheral neuropathy under electrical stimulation. Bioactive Materials, 2021, 6,<br>2231-2249.                       | 15.6 | 36        |
| 46 | Optical and gamma-ray shielding effectiveness of a newly fabricated P2O5–CaO–Na2O–K2O–PbO glass system. Progress in Nuclear Energy, 2021, 138, 103798.   | 2.9  | 20        |
| 47 | Effect of Add-On Therapy of Dapagliflozin and Empagliflozin on Adipokines in Type 2 Diabetes Mellitus.<br>Journal of Endocrinology and Metabolism, 2021, 11, 83-90.  | 0.4  | 1         |
| 48 | Evaluation of optical, and radiation shielding features of New phosphate-based glass system. Optik, 2021, 242, 167220.   | 2.9  | 24        |
| 49 | Experimental Investigation of Radiation Shielding Competence of Bi2O3-CaO-K2O-Na2O-P2O5 Glass Systems. Materials, 2021, 14, 5061.  | 2.9  | 33        |
| 50 | Mechanical and photon shielding aspects of PbO–BaO–WO3–Na2O–B2O3 glass systems. Applied<br>Physics A: Materials Science and Processing, 2021, 127, 1.  | 2.3  | 10        |
| 51 | Nanocrystallite assembled La2CoNiO6 nanorods fabricated by facile solvothermal route for electrochemical performance. Journal of Nanoparticle Research, 2021, 23, 1.   | 1.9  | 1         |
| 52 | Implementation of stacking based ARIMA model for prediction of Covid-19 cases in India. Journal of Biomedical Informatics, 2021, 121, 103887.  | 4.3  | 38        |
| 53 | Gamma-ray shielding, physical, and structural characteristics of TeO2–CdO–PbO–B2O3 glasses.<br>Optical Materials, 2021, 119, 111333.   | 3.6  | 14        |
| 54 | Optical, mechanical properties of TeO2-CdO-PbO-B2O3 glass systems and radiation shielding investigation using EPICS2017 library. Optik, 2021, 242, 167342.   | 2.9  | 58        |

Ashok Kumar

| #  | Article  | IF  | CITATIONS |
|----|--|-----|-----------|
| 55 | Investigation of the optical, mechanical, and radiation shielding features for strontium-borotellurite glass system: Fabrication, characterization, and EPICS2017 computations. Optik, 2021, 243, 167468.                        | 2.9 | 18        |
| 56 | The physical, structural and the gamma ray shielding effectiveness of the novel Li2O-K2O–B2O3–TeO2 glasses. Results in Physics, 2021, 29, 104726.  | 4.1 | 18        |
| 57 | A Prospective Study of Novel Therapeutic Targets Interleukin 6, Tumor Necrosis Factor α, and<br>Interferon γ as Predictive Biomarkers for the Development of Posttraumatic Epilepsy. World<br>Neurosurgery: X, 2021, 12, 100107. | 1.1 | 6         |
| 58 | Dielectric constant, polarizability, susceptibility and gamma ray shielding behavior of the<br>Li2O-Li2MoO4-TiO2-P2O5 glasses. Optik, 2021, 245, 167639.   | 2.9 | 4         |
| 59 | Experimental and theoretical analysis of radiation shielding properties of strontium-borate-tellurite glasses. Optical Materials, 2021, 121, 111589.   | 3.6 | 28        |
| 60 | A novel CaO–K2O–Na2O–P2O5 glass systems for radiation shielding applications. Radiation Physics<br>and Chemistry, 2021, 188, 109645.   | 2.8 | 48        |
| 61 | SrO-SiO2-B2O3-ZrO2 glass system: Effects of varying SrO and BaO compositions to physical and optical properties, and radiation shielding using EPDL2017 photoatomic library. Optik, 2021, 245, 167670.                           | 2.9 | 14        |
| 62 | Optical and gamma ray shielding properties BaO doped K2O-TiO2-P2O5 glasses. Optik, 2021, 247, 167893.  | 2.9 | 0         |
| 63 | Effect of adding SrO, TeO2, PbO, and Bi2O3 heavy metal oxides on the optical and gamma ray shielding properties of Li2O-K2O-B2O3 glasses. Optik, 2021, 247, 167848.  | 2.9 | 3         |
| 64 | Li2O-K2O-B2O3-PbO glass system: Optical and gamma-ray shielding investigations. Optik, 2021, 247, 167792.  | 2.9 | 39        |
| 65 | B2O3-TeO2-K2O-Li2O glasses: Optical and gamma ray shielding characterization. Optik, 2021, 247, 167847.  | 2.9 | 0         |
| 66 | LiKBPbX glasses: Physical, structural and gamma ray shielding competence. Optik, 2021, 247, 167835.  | 2.9 | 1         |
| 67 | Intra-articular gold induced cytokine (GOLDIC®) injection therapy in patients with osteoarthritis of knee joint: a clinical study. International Orthopaedics, 2021, 45, 497-507.  | 1.9 | 14        |
| 68 | Structural, dielectric and magnetic properties of double perovskite-La2CoNiO6 ceramics synthesised by wet chemical route. International Journal of Nanotechnology, 2021, 18, 622.  | 0.2 | 1         |
| 69 | Current strategies in tailoring methods for engineered exosomes and future avenues in biomedical applications. Journal of Materials Chemistry B, 2021, 9, 6281-6309.   | 5.8 | 21        |
| 70 | Gamma ray interaction studies of the PbCl2–SnCl2–P2O5 bioactive glass system for applications in nuclear medicine. Journal of the Australian Ceramic Society, 2021, 57, 635-642.   | 1.9 | 5         |
| 71 | Impact of Renewable Energy Sources into Multi Area Multi-Source Load Frequency Control of<br>Interrelated Power System. Mathematics, 2021, 9, 186.   | 2.2 | 21        |
| 72 | Impact of replacement of B2O3 by TeO2 on the physical, optical and gamma ray shielding<br>characteristics of Pb-free B2O3-TeO2-ZnO-Al2O3-Li2O-MgO glass system. Optik, 2021, 248, 168100.  | 2.9 | 1         |

| #  | Article  | IF                 | CITATIONS                              |
|----|--|--------------------|--|
| 73 | H19Xâ€encoded miRâ€322(424)/miRâ€503 regulates muscle mass by targeting translation initiation factors.<br>Journal of Cachexia, Sarcopenia and Muscle, 2021, 12, 2174-2186.                        | 7.3                | 9                                      |
| 74 | Impact of Bi2O3 on optical properties and radiation attenuation characteristics of Bi2O3-Li2O-P2O5 glasses. Optik, 2021, 248, 168081.  | 2.9                | 8                                      |
| 75 | Exploration of the B2O3-Bi2O3-MoO3 glass system based on its physical, optical, and gamma ray shielding capabilities. Optik, 2021, 248, 168177.  | 2.9                | 2                                      |
| 76 | Evaluation of structural and gamma ray shielding competence of Li2O-K2O-B2O3-HMO (HMO =) Tj ETQq0 0 0 rg   | gBT_/Overlo<br>2.9 | $\operatorname{pck}_{30}^{10}$ Tf 50 6 |
| 77 | ACE2 Expression in the Pancreas and Association With COVID-19 Infection. Pancreas, 2021, 50, e1-e2.  | 1.1                | 3                                      |
| 78 | Comparison of Ultrasonography and X-Rays for the Diagnosis of Synovitis and Bony Erosions in Small<br>Joints of Hands in Early Rheumatoid Arthritis: a Prospective Study. Mædica, 2021, 16, 22-28. | 0.1                | 0                                      |
| 79 | The IRE1/XBP1 signaling axis promotes skeletal muscle regeneration through a cell non-autonomous mechanism. ELife, 2021, 10, .   | 6.0                | 11                                     |
| 80 | Illustration of distinct nuclear radiation transmission factors combined with physical and elastic characteristics of barium boro-bismuthate glasses. Results in Physics, 2021, 31, 105067.        | 4.1                | 26                                     |
| 81 | Therapeutic plasma exchange in acute fatty liver of pregnancy: a case report and literature review. Pan<br>African Medical Journal, 2021, 40, 220.   | 0.8                | 2                                      |
| 82 | An Offset CPW-Fed Dual-Band Circularly Polarized Printed Antenna for Multiband Wireless<br>Applications. Lecture Notes in Electrical Engineering, 2020, , 411-418.                                 | 0.4                | 7                                      |
| 83 | Design and Studies of Bandstop Filters Using Modified CSRR DGS for WLAN Applications. Lecture Notes in Electrical Engineering, 2020, , 467-475.  | 0.4                | 3                                      |
| 84 | Experimental studies and Monte Carlo simulations on gamma ray shielding competence of (30+x)PbO<br>10WO3 10Na2Oâ€`â^`â€~10MgO – (40-x)B2O3 glasses. Progress in Nuclear Energy, 2020, 119, 103047. | 2.9                | 93                                     |

| 85 | Shielding behaviour of (20â€ <sup>-</sup> +â€ <sup>-</sup> x) Bi2O3 – 20BaO–10Na2O–10MgO–(40-x) B2O3: An experimental an Carlo study. Chemical Physics, 2020, 529, 110571. | d Monte<br>1.9 | 42  |
|----|--|----------------|-----|
| 86 | Nanohydroxyapatite Based Ceramic Carrier Promotes Bone Formation in a Femoral Neck Canal Defect<br>in Osteoporotic Rats. Biomacromolecules, 2020, 21, 328-337.             | 5.4            | 40  |
| 87 | Surface modification of reduced graphene oxideâ€polyaniline nanotubes nanocomposites for improved supercapacitor electrodes. Polymer Composites, 2020, 41, 653-667.        | 4.6            | 15  |
| 88 | Evaluation of gamma-ray and neutron shielding features of heavy metals doped<br>Bi2O3-BaO-Na2O-MgO-B2O3 glass systems. Progress in Nuclear Energy, 2020, 118, 103118.      | 2.9            | 102 |
| 89 | Response to a Fire Incident in the Operation Room: A Cautionary Tale. Disaster Medicine and Public<br>Health Preparedness, 2020, 14, 284-288.                              | 1.3            | 7   |
|    | Gelatin interpenetration in poly N â€isopropylacrylamide network reduces the compressive modulus of  |                |     |

the scaffold: A property employed to mimic hepatic matrix stiffness. Biotechnology and
3.3
Bioengineering, 2020, 117, 567-579.

| #   | Article  | IF  | CITATIONS |
|-----|--|-----|-----------|
| 91  | Effect of MnO on structural, optical and thermoluminescence properties of lithium borosilicate glasses. Journal of Luminescence, 2020, 219, 116872.  | 3.1 | 20        |
| 92  | Probing the ionic transport dynamics in ionic liquid incorporated CuBTC-Metal-Organic Framework based PVdF-HFP nanocomposite membranes. Solid State Sciences, 2020, 100, 106115.   | 3.2 | 14        |
| 93  | Role of surfactant in optimization of 3D ZnO floret as photoanode for dye sensitized solar cell.<br>Applied Nanoscience (Switzerland), 2020, 10, 1035-1044.  | 3.1 | 2         |
| 94  | Comparative study of gamma-ray shielding features and some properties of different heavy metal oxide-based tellurite-rich glass systems. Radiation Physics and Chemistry, 2020, 170, 108633.   | 2.8 | 17        |
| 95  | Microstructure and electrochemical performance of La2ZnMnO6 nanoflakes synthesized by facile hydrothermal route. Applied Physics A: Materials Science and Processing, 2020, 126, 1.  | 2.3 | 28        |
| 96  | Wet chemical synthesis and electrochemical performance of novel double perovskite Y2CuMnO6 nanocrystallites. Materials Science in Semiconductor Processing, 2020, 107, 104826.   | 4.0 | 22        |
| 97  | Adipose-Derived Stem Cells (ADSCs) Loaded Gelatin-Sericin-Laminin Cryogels for Tissue Regeneration in<br>Diabetic Wounds. Biomacromolecules, 2020, 21, 294-304.  | 5.4 | 37        |
| 98  | Theoretical and experimental validation gamma shielding properties of B2O3–ZnO–MgO–Bi2O3 glass<br>system. Materials Chemistry and Physics, 2020, 242, 122504.  | 4.0 | 36        |
| 99  | Wideband circularly polarized parasitic patches loaded coplanar waveguide-fed square slot antenna<br>with grounded strips and slots for wireless communication systems. AEU - International Journal of<br>Electronics and Communications, 2020, 114, 153011. | 2.9 | 18        |
| 100 | Local and Sustained Delivery of Rifampicin from a Bioactive Ceramic Carrier Treats Bone Infection in<br>Rat Tibia. ACS Infectious Diseases, 2020, 6, 2938-2949.  | 3.8 | 26        |
| 101 | Reckoning of nuclear radiation attenuation capabilities for binary GeO2-Tl2O, GeO2-Bi2O3, and ternary GeO2-Tl2O–Bi2O3 glasses utilizing pertinent theoretical and computational approaches. Optical Materials, 2020, 108, 110113.                            | 3.6 | 10        |
| 102 | Dextran based amphiphilic nano-hybrid hydrogel system incorporated with curcumin and cerium oxide nanoparticles for wound healing. Colloids and Surfaces B: Biointerfaces, 2020, 195, 111263.  | 5.0 | 84        |
| 103 | Redispersion of cryoaggregated gold nanoparticle by means of laser irradiation and effect on biological interactions. Nanotechnology, 2020, 31, 435601.  | 2.6 | 1         |
| 104 | Letter to the editor in response to COVID-19 presenting as acute pancreatitis. Pancreatology, 2020, 20, 1021-1022.   | 1.1 | 7         |
| 105 | Phase transformation in wet chemically synthesized Y2NiFeO6, and its magnetic and energy storage properties. Applied Physics A: Materials Science and Processing, 2020, 126, 1.  | 2.3 | 6         |
| 106 | SnO-reinforced silicate glasses and utilization in gamma-radiation-shielding applications. Emerging<br>Materials Research, 2020, 9, 1000-1008.   | 0.7 | 67        |
| 107 | Investigation of structural, morphological and electrochemical properties of mesoporous<br>La2CuCoO6 rods fabricated by facile hydrothermal route. International Journal of Minerals,<br>Metallurgy and Materials, 2020, 27, 987-995.                        | 4.9 | 12        |
| 108 | Facile solvothermal synthesis of nano-assembled mesoporous rods of cobalt free – La2NiFeO6 for<br>electrochemical behaviour. Materials Science and Engineering B: Solid-State Materials for Advanced<br>Technology, 2020, 261, 114664.                       | 3.5 | 11        |

| #   | Article   | IF          | CITATIONS |
|-----|---|-------------|-----------|
| 109 | Binary B2O3–Bi2O3 glasses: scrutinization of directly and indirectly ionizing radiations shielding abilities. Journal of Materials Research and Technology, 2020, 9, 14549-14567.   | 5.8         | 63        |
| 110 | Coronavirus disease 2019 and the pancreas. Pancreatology, 2020, 20, 1567-1575.  | 1.1         | 49        |
| 111 | Agar–Iodine Transdermal Patches for Infected Diabetic Wounds. ACS Applied Bio Materials, 2020, 3,<br>7515-7530.   | 4.6         | 14        |
| 112 | Feasibility of telemedicine in maintaining follow-up of orthopaedic patients and their satisfaction: A preliminary study. Journal of Clinical Orthopaedics and Trauma, 2020, 11, S704-S710.   | 1.5         | 46        |
| 113 | Structural, Dielectric, and Energy Storage Properties of Citric Acid and Ethylene Glycol Assisted<br>Hydrothermally Synthesized Y <sub>2</sub> FeCoO <sub>6</sub> . Physica Status Solidi (A) Applications<br>and Materials Science, 2020, 217, 2000324.                      | 1.8         | 6         |
| 114 | A study of critical minima and spin polarization in the e±–Ba elastic scattering. European Physical<br>Journal D, 2020, 74, 1.  | 1.3         | 5         |
| 115 | Data supporting exosome laden oxygen releasing antioxidant and antibacterial cryogel wound dressing OxOBand alleviate diabetic and infectious wound healing. Data in Brief, 2020, 31, 105671.   | 1.0         | 16        |
| 116 | Perioperative COVID-19 testing for orthopaedic patients: Current evidence. Journal of Clinical Orthopaedics and Trauma, 2020, 11, S296-S297.  | 1.5         | 5         |
| 117 | Structural, optical and thermoluminescence properties of newly developed MnKB: Er3+ glass system.<br>Journal of Non-Crystalline Solids, 2020, 543, 120113.  | 3.1         | 17        |
| 118 | Optimization Methodologies and Testing on Standard Benchmark Functions of Load Frequency<br>Control for Interconnected Multi Area Power System in Smart Grids. Mathematics, 2020, 8, 980.   | 2.2         | 14        |
| 119 | Oxidised charcoal: an efficient support for NiFe layered double hydroxide to improve electrochemical oxygen evolution. Chemical Communications, 2020, 56, 8770-8773.  | 4.1         | 10        |
| 120 | Mesoporous spheres of Dy2NiMnO6 synthesized via hydrothermal route for structural, morphological, and electrochemical investigation. Ionics, 2020, 26, 5143-5153.   | 2.4         | 12        |
| 121 | Biofabrication of gold nanoparticles with bone remodeling potential: an in vitro and in vivo assessment. Journal of Nanoparticle Research, 2020, 22, 1.   | 1.9         | 10        |
| 122 | Neuroprotective Role of Oral Vitamin D Supplementation on Consciousness and Inflammatory<br>Biomarkers in Determining Severity Outcome in Acute Traumatic Brain Injury Patients: A Double-Blind<br>Randomized Clinical Trial. Clinical Drug Investigation, 2020, 40, 327-334. | 2.2         | 28        |
| 123 | Li2O–B2O3–Bi2O3 glasses: gamma-rays and neutrons attenuation study using ParShield/WinXCOM<br>program and Geant4 and Penelope codes. Applied Physics A: Materials Science and Processing, 2020, 126,<br>1.  | 2.3         | 14        |
| 124 | The synthesis, structural, optical and electrical characterizations of double perovskite oxide<br>Y2CuCoO5. AIP Conference Proceedings, 2020, , .   | 0.4         | 0         |
| 125 | TAK1 preserves skeletal muscle mass and mitochondrial function through redox homeostasis. FASEB<br>BioAdvances, 2020, 2, 538-553.   | 2.4         | 11        |
| 126 | B2O3–Bi2O3–TeO2–BaO and TeO2–Bi2O3–BaO glass systems: a comparative assessment of gamma and fast and thermal neutron attenuation aspects. Applied Physics A: Materials Science and Processing, 2020, 126, 1.  | -ray<br>2.3 | 69        |

| #   | Article   | IF  | CITATIONS |
|-----|---|-----|-----------|
| 127 | Structural, Optical, and Multiferroic Properties of Yttrium (Y3+)-Substituted BiFeO3 Nanostructures.<br>Journal of Superconductivity and Novel Magnetism, 2020, 33, 2017-2029.  | 1.8 | 9         |
| 128 | Structural and multiferroic properties of BiFeO3/MgLa0.025Fe1.975O4 nanocomposite synthesized by sol–gel auto combustion route. Journal of Materials Science: Materials in Electronics, 2020, 31, 2777-2788.                          | 2.2 | 8         |
| 129 | Solvothermal synthesis dependent structural, morphological and electrochemical behaviour of mesoporous nanorods of Sm2NiMnO6. Ceramics International, 2020, 46, 11041-11048.  | 4.8 | 20        |
| 130 | Asymmetric CPW-Fed Multistubs Loaded Compact Printed Multiband Antenna for Wireless Applications. Lecture Notes in Electrical Engineering, 2020, , 317-324.   | 0.4 | 0         |
| 131 | Investigation of Substrate Integrated Waveguide (SIW) Filter Using Defected Ground Structure (DGS).<br>Lecture Notes in Electrical Engineering, 2020, , 449-456.  | 0.4 | 0         |
| 132 | Performance Analysis of Underwater 2D OCDMA System. Lecture Notes in Electrical Engineering, 2020, , 477-484.   | 0.4 | 6         |
| 133 | Studies of Various Artificial Magnetic Conductor for 5G Applications. Lecture Notes in Electrical Engineering, 2020, , 523-530.   | 0.4 | 4         |
| 134 | Broadband Circularly Polarized CPW-Fed Inverted-L Grounded Strips and SRR Loaded Square Slot<br>Antenna for Wi-Fi/WiMAX/5G Applications. Lecture Notes in Electrical Engineering, 2020, , 591-596.                                    | 0.4 | 0         |
| 135 | TeO2–B2O3–ZnO–La2O3 glasses: γ-ray and neutron attenuation characteristics analysis by WinXCOM program, MCNP5, Geant4, and Penelope simulation codes. Ceramics International, 2020, 46, 16620-16635.                                  | 4.8 | 27        |
| 136 | Energy storage properties of double perovskites Gd2NiMnO6 for electrochemical supercapacitor application. Solid State Sciences, 2020, 105, 106252.  | 3.2 | 34        |
| 137 | Ethylene glycol/citric acid stabilized wet chemically synthesized Y2CoNiO6, and its structural,<br>dielectric, magnetic and electrochemical behavior. Journal of Materials Science: Materials in<br>Electronics, 2020, 31, 6977-6987. | 2.2 | 16        |
| 138 | The role of PbO/Bi2O3 insertion on the shielding characteristics of novel borate glasses. Ceramics International, 2020, 46, 23357-23368.  | 4.8 | 83        |
| 139 | Enhanced bone mineralization using hydroxyapatite-based ceramic bone substitute<br>incorporating <i>Withania somnifera</i> extracts. Biomedical Materials (Bristol), 2020, 15, 055015.  | 3.3 | 15        |
| 140 | Zn Doped α-Fe2O3: An Efficient Material for UV Driven Photocatalysis and Electrical Conductivity.<br>Crystals, 2020, 10, 273.   | 2.2 | 86        |
| 141 | Structural and paramagnetic resonance properties correlation in lanthanum ion doped nickel ferrite nanoparticles. Journal of Magnetism and Magnetic Materials, 2020, 508, 166866.   | 2.3 | 18        |
| 142 | Improved Bone Regeneration in Rabbit Bone Defects Using 3D Printed Composite Scaffolds<br>Functionalized with Osteoinductive Factors. ACS Applied Materials & Interfaces, 2020, 12,<br>48340-48356.                                   | 8.0 | 23        |
| 143 | Prevalence and risk factors for nonalcoholic fatty liver disease in obese children in rural Punjab,<br>India. Journal of Family and Community Medicine, 2020, 27, 103.  | 1.1 | 9         |
| 144 | Management of hunger strike: A medical, ethical and legal conundrum. Medico-Legal Journal, 2020, 88,<br>215-219.  | 0.5 | 0         |

| #   | Article  | IF  | CITATIONS |
|-----|--|-----|-----------|
| 145 | Loss of seed viability in onion (Allium cepa L.) in relation to degradation of lipids during storage.<br>Journal of Applied and Natural Science, 2020, 12, 635-640.  | 0.4 | 2         |
| 146 | Ripple-Free Input Current High Voltage Gain DC–DC Converters With Coupled Inductors. IEEE<br>Transactions on Power Electronics, 2019, 34, 3418-3428.   | 7.9 | 67        |
| 147 | Size dependent morphology, magnetic and dielectric properties of BiFeO3 nanoparticles. MRS<br>Advances, 2019, 4, 1659-1665.  | 0.9 | 7         |
| 148 | Effect of novel ZnO/Zn2SnO4 photoanode on the performance of dye sensitized solar cell. Optik, 2019, 194, 163117.  | 2.9 | 21        |
| 149 | Physiological Biomimetic Culture System for Pig and Human Heart Slices. Circulation Research, 2019, 125, 628-642.  | 4.5 | 60        |
| 150 | MINIATURIZED MULTISTUBS LOADED RECTANGULAR MONOPOLE ANTENNA FOR MULTIBAND APPLICATIONS<br>BASED ON THEORY OF CHARACTERISTICS MODES. Progress in Electromagnetics Research C, 2019, 92,<br>177-189.                                     | 0.9 | 7         |
| 151 | Structural, optical, and gamma-ray-sensing characterization of (35Ââ^'Âx) PbO–10 MgO–10Na2O–5<br>Fe2O3–10 BaO–(30Ââ^'Âx) B2O3 glasses. Applied Physics A: Materials Science and Processing, 2019, 125, 1.                              | 2.3 | 13        |
| 152 | Dual wideband circular polarized CPW-fed strip and slots loaded compact square slot antenna for wireless and satellite applications. AEU - International Journal of Electronics and Communications, 2019, 108, 181-188.                | 2.9 | 32        |
| 153 | Hydrothermal synthesis and electrochemical performance of nanostructured cobalt free<br>La2CuMnO6. Solid State Sciences, 2019, 95, 105927.   | 3.2 | 31        |
| 154 | Morphology correlated efficiency of ZnO photoanode in dye sensitized solar cell. Materials Research<br>Express, 2019, 6, 1050d3.   | 1.6 | 4         |
| 155 | Assessment of gamma-rays and fast neutron beam attenuation features of Er2O3-doped<br>B2O3–ZnO–Bi2O3 glasses using XCOM and simulation codes (MCNP5 and Geant4). Applied Physics A:<br>Materials Science and Processing, 2019, 125, 1. | 2.3 | 17        |
| 156 | Gamma ray shielding behavior of Li2O-doped PbO–MoO3–B2O3 glass system. Applied Physics A:<br>Materials Science and Processing, 2019, 125, 1.   | 2.3 | 18        |
| 157 | Optically transparent newly developed glass materials for gamma ray shielding applications. Journal of Non-Crystalline Solids, 2019, 521, 119490.  | 3.1 | 15        |
| 158 | Extensive study of newly developed highly dense transparent PbO-WO3-BaO-Na2O-B2O3 glasses for radiation shielding applications. Journal of Non-Crystalline Solids, 2019, 521, 119521.  | 3.1 | 19        |
| 159 | Investigations on magnetic and electrical properties of Zn doped Fe2O3 nanoparticles and their correlation with local electronic structures. Journal of Magnetism and Magnetic Materials, 2019, 489, 165398.                           | 2.3 | 36        |
| 160 | The Toll-Like Receptor/MyD88/XBP1 Signaling Axis Mediates Skeletal Muscle Wasting during Cancer<br>Cachexia. Molecular and Cellular Biology, 2019, 39, .   | 2.3 | 37        |
| 161 | Elastic scattering of electrons by Sr atom: a study of critical minima and spin polarization. Journal of Physics Communications, 2019, 3, 065001.  | 1.2 | 4         |
| 162 | A novel single myocapsular sleeve (SMS) repair technique to reduce dislocation in posterior approach<br>to the hip: A clinico-radiographic study. Journal of Clinical Orthopaedics and Trauma, 2019, 10,<br>S247-S251.                 | 1.5 | 0         |

| #   | Article  | IF  | CITATIONS |
|-----|--|-----|-----------|
| 163 | Boro-silicate glasses co-doped Er+3/Yb+3 for optical amplifier and gamma radiation shielding applications. Physica B: Condensed Matter, 2019, 567, 37-44.  | 2.7 | 42        |
| 164 | Influence of La3+ ion doping on structural and magnetic properties of nickel ferrite nanoparticles prepared by sol-gel route. AIP Conference Proceedings, 2019, , .  | 0.4 | 2         |
| 165 | Chitosan-Gelatin-Polypyrrole Cryogel Matrix for Stem Cell Differentiation into Neural Lineage and Sciatic Nerve Regeneration in Peripheral Nerve Injury Model. ACS Biomaterials Science and Engineering, 2019, 5, 3007-3021.         | 5.2 | 23        |
| 166 | Facile synthesis of novel ZnO/Cd0.5Zn0.5S photoanode for dye-sensitized solar cell. Materials<br>Research Express, 2019, 6, 085029.  | 1.6 | 4         |
| 167 | Electrochemical behavior of oxygen-deficient double perovskite, Ba2FeCoO6-δ, synthesized by facile wet<br>chemical process. Ceramics International, 2019, 45, 14105-14110.   | 4.8 | 30        |
| 168 | 100 MeV O <sup>7+</sup> ion irradiation induced electrochemical enhancement in NiBTC metal-organic<br>framework based composite polymer electrolytes incorporated with ionic liquid. Materials Research<br>Express, 2019, 6, 085305. | 1.6 | 4         |
| 169 | Studies on the structural, optical and radiation shielding properties of (50 – x) PbO – 10 WO3–10<br>Na2O – 10 MgO – (20†+†x) B2O3 glasses. Journal of Non-Crystalline Solids, 2019, 513, 159-166.                                   | 3.1 | 36        |
| 170 | Facile wet chemical synthesis and electrochemical behavior of La2FeCoO6 nano-crystallites. Materials Science in Semiconductor Processing, 2019, 99, 8-13.  | 4.0 | 31        |
| 171 | Scope of Artificial Intelligence for Interconnected Multi Area Power System: A Literature Review. , 2019, , .  |     | Ο         |
| 172 | A Cascaded Buck-Flyback Structure for High Voltage Step Down Applications. , 2019, , .   |     | 4         |
| 173 | Scope of Meta-Heuristics Optimizer for Automatic Generation Control of Realistic Power System. , 2019, , .   |     | 1         |
| 174 | Operating Modes based Review of Single-Stage Buck-Boost Inverters. , 2019, , .   |     | 2         |
| 175 | ER Stress and Unfolded Protein Response in Cancer Cachexia. Cancers, 2019, 11, 1929.   | 3.7 | 40        |
| 176 | Influence of Ce3+ Ion Doping on Structural and Magnetic Properties of Magnesium Nanoferrite.<br>Journal of Superconductivity and Novel Magnetism, 2019, 32, 1465-1474.   | 1.8 | 11        |
| 177 | PERK regulates skeletal muscle mass and contractile function in adult mice. FASEB Journal, 2019, 33, 1946-1962.  | 0.5 | 45        |
| 178 | Physical, structural, optical and thermoluminescence behavior of Dy2O3 doped sodium magnesium borosilicate glasses. Results in Physics, 2019, 12, 827-839.   | 4.1 | 67        |
| 179 | Effects of different concentration and combinations of cryoprotectants on sperm quality, functional integrity in three Indian horse breeds. Cryobiology, 2019, 86, 52-57.  | 0.7 | 19        |
| 180 | Composite bilayered scaffolds with bio-functionalized ceramics for cranial bone defects: An <i>in vivo</i> evaluation. Multifunctional Materials, 2019, 2, 014002.   | 3.7 | 5         |

Ashok Kumar

| #   | Article  | IF  | CITATIONS |
|-----|--|-----|-----------|
| 181 | Mixed transition and rare earth ion doped borate glass: structural, optical and thermoluminescence study. Journal of Materials Science: Materials in Electronics, 2019, 30, 677-686.   | 2.2 | 32        |
| 182 | Aligned Chitosan-Gelatin Cryogel-Filled Polyurethane Nerve Guidance Channel for Neural Tissue<br>Engineering: Fabrication, Characterization, and In Vitro Evaluation. Biomacromolecules, 2019, 20,<br>662-673.                           | 5.4 | 69        |
| 183 | Quality assurance and adverse event management in regenerative medicine for knee osteoarthritis:<br>Current concepts. Journal of Clinical Orthopaedics and Trauma, 2019, 10, 53-58.  | 1.5 | 8         |
| 184 | Comparative study of structural, magnetic and dielectric properties of CoFe2O4 @ BiFeO3 and<br>BiFeO3@ CoFe2O4 core-shell nanocomposites. Journal of Magnetism and Magnetic Materials, 2019, 475,<br>30-37.                              | 2.3 | 29        |
| 185 | Canonical NF-κB signaling regulates satellite stem cell homeostasis and function during regenerative<br>myogenesis. Journal of Molecular Cell Biology, 2019, 11, 53-66.  | 3.3 | 19        |
| 186 | Physical, structural, optical and gamma ray shielding behavior of (20+x) PbO – 10 BaO – 10 Na2O – 10<br>MgO – (50-x) B2O3 glasses. Physica B: Condensed Matter, 2019, 552, 110-118.  | 2.7 | 102       |
| 187 | <scp>ER</scp> stress in skeletal muscle remodeling and myopathies. FEBS Journal, 2019, 286, 379-398.   | 4.7 | 96        |
| 188 | Endogenous Platelet-Rich Plasma Supplements/Augments Growth Factors Delivered via Porous<br>Collagen-Nanohydroxyapatite Bone Substitute for Enhanced Bone Formation. ACS Biomaterials<br>Science and Engineering, 2019, 5, 56-69.        | 5.2 | 19        |
| 189 | Perceived effectiveness of infection control practices in Laundry of a tertiary healthcare centre.<br>World Journal of Emergency Medicine, 2019, 10, 114.  | 1.0 | 1         |
| 190 | Mechanical and gamma-ray shielding properties of TeO2-ZnO-NiO glasses. Materials Chemistry and Physics, 2018, 212, 12-20.  | 4.0 | 100       |
| 191 | Miniaturized wideband dual linearly and circularly polarized printed square slot antenna for<br>multiradio wireless systems. AEU - International Journal of Electronics and Communications, 2018, 88,<br>44-51.                          | 2.9 | 30        |
| 192 | Facile wet chemical synthesis of Er3+/Yb3+ co-doped BaSnO3 nano-crystallites for dye-sensitized solar cell application. Materials Science in Semiconductor Processing, 2018, 83, 83-88.  | 4.0 | 30        |
| 193 | A novel long non-coding RNA Myolinc regulates myogenesis through TDP-43 and Filip1. Journal of<br>Molecular Cell Biology, 2018, 10, 102-117.   | 3.3 | 56        |
| 194 | Comparative study of gamma ray shielding competence of WO 3 -TeO 2 -PbO glass system to different glasses and concretes. Materials Chemistry and Physics, 2018, 213, 508-517.  | 4.0 | 140       |
| 195 | An offset CPW-fed triple-band circularly polarized printed antenna for multiband wireless<br>applications. AEU - International Journal of Electronics and Communications, 2018, 86, 133-141.   | 2.9 | 25        |
| 196 | Frequency Domain Analysis and Optimal Design of Isolated Bidirectional Series Resonant Converter.<br>IEEE Transactions on Industry Applications, 2018, 54, 356-366.  | 4.9 | 32        |
| 197 | Cetyltriammonium Bromide Assisted Synthesis of Lanthanum Containing Barium Stannate<br>Nanoparticles for Application in Dye Sensitized Solar Cells. Physica Status Solidi (A) Applications and<br>Materials Science, 2018, 215, 1700723. | 1.8 | 19        |
| 198 | Behavior of lanthanum containing barium stannate nanoparticles synthesized by cetyltriammonium bromide assisted wet chemistry route. Materials Research Express, 2018, 5, 025030.  | 1.6 | 1         |

| #   | Article  | IF   | CITATIONS |
|-----|--|------|-----------|
| 199 | Compact Triple-Band Stubs-Loaded Rectangular Monopole Antenna for WiMAX/WLAN Applications.<br>Lecture Notes in Electrical Engineering, 2018, , 429-435.  | 0.4  | 3         |
| 200 | Engineering Bioinspired Antioxidant Materials Promoting Cardiomyocyte Functionality and<br>Maturation for Tissue Engineering Application. ACS Applied Materials & Interfaces, 2018, 10,<br>3260-3273.  | 8.0  | 68        |
| 201 | Design of multiâ€polarised quadâ€band planar antenna with parasitic multistubs for multiband wireless<br>communication. IET Microwaves, Antennas and Propagation, 2018, 12, 718-726.   | 1.4  | 22        |
| 202 | Emerging roles of ER stress and unfolded protein response pathways in skeletal muscle health and disease. Journal of Cellular Physiology, 2018, 233, 67-78.  | 4.1  | 135       |
| 203 | A novel method of utilization of hot dip galvanizing slag using the heat waste from itself for protection from radiation. Journal of Hazardous Materials, 2018, 344, 602-614.  | 12.4 | 55        |
| 204 | Thermal, electrical, and dielectric properties of reduced graphene oxide–polyaniline nanotubes hybrid<br>nanocomposites synthesized by <i>in situ</i> reduction and varying graphene oxide concentration.<br>Journal of Applied Polymer Science, 2018, 135, 45883. | 2.6  | 22        |
| 205 | Cetyltrimethyl ammonium bromide stabilized lanthanum doped SrSnO3 nanoparticle photoanode for dye sensitized solar cell application. Solid State Communications, 2018, 269, 6-10.  | 1.9  | 14        |
| 206 | New Switching Strategy for Single-Mode Operation of a Single-Stage Buck–Boost Inverter. IEEE<br>Transactions on Power Electronics, 2018, 33, 5927-5936.  | 7.9  | 24        |
| 207 | Effect of PbO on the shielding behavior of ZnO–P2O5 glass system using Monte Carlo simulation.<br>Journal of Non-Crystalline Solids, 2018, 481, 604-607.   | 3.1  | 51        |
| 208 | Decellularized Liver Matrix-Modified Cryogel Scaffolds as Potential Hepatocyte Carriers in<br>Bioartificial Liver Support Systems and Implantable Liver Constructs. ACS Applied Materials &<br>Interfaces, 2018, 10, 114-126.                                      | 8.0  | 53        |
| 209 | Exploration of gamma radiation shielding features for titanate bismuth borotellurite glasses using<br>relevant software program and Monte Carlo simulation code. Journal of Non-Crystalline Solids, 2018,<br>481, 65-73.   | 3.1  | 57        |
| 210 | TAK1 regulates skeletal muscle mass and mitochondrial function. JCI Insight, 2018, 3, .  | 5.0  | 38        |
| 211 | Inner Loop Stability of Peak Current Controlled Cuk and SEPIC Converters. , 2018, , .  |      | 2         |
| 212 | Derivation of Single-Stage Single-Phase Fourth Order Buck-boost Inverters. , 2018, , .   |      | 2         |
| 213 | CCM-DCM Operation of a High Voltage Gain Boost-Flyback Derived Converter. , 2018, , .  |      | 1         |
| 214 | Two High Voltage Gain Non-isolated Dc-dc Converters with Ripple Free Input Current. , 2018, , .  |      | 0         |
| 215 | Biomimetic Photocurable Three-Dimensional Printed Nerve Guidance Channels with Aligned<br>Cryomatrix Lumen for Peripheral Nerve Regeneration. ACS Applied Materials & Interfaces, 2018, 10,<br>43327-43342.  | 8.0  | 62        |
| 216 | Radiation shielding parameters of BaO–Nb <sub>2</sub> O <sub>5</sub> –P <sub>2</sub> O <sub>5</sub><br>glass system using MCNP5 code and XCOM software. Materials Research Express, 2018, 5, 115203.   | 1.6  | 15        |

| #   | Article   | IF  | CITATIONS |
|-----|---|-----|-----------|
| 217 | Amine-Functionalized Electrically Conductive Core–Sheath MEH-PPV:PCL Electrospun Nanofibers for<br>Enhanced Cell–Biomaterial Interactions. ACS Biomaterials Science and Engineering, 2018, 4, 3327-3346.  | 5.2 | 24        |
| 218 | Annealing effect on the structural and dielectric properties of hematite nanoparticles. AIP Conference Proceedings, 2018, , .   | 0.4 | 11        |
| 219 | Nickel-induced magnetic behaviour of nano-structured α-Fe <sub>2</sub> O <sub>3</sub> , synthesised by facile wet chemical route. Philosophical Magazine, 2018, 98, 2425-2439.  | 1.6 | 6         |
| 220 | Gamma ray shielding studies on 26.66<br>B <sub>2</sub> O <sub>3</sub> –16GeO <sub>2</sub> –4Bi <sub>2</sub> O <sub>3</sub> –(53.33–x)<br>PbO–xPbF <sub>2</sub> glass system using MCNPX, Geant4 and XCOM. Materials Research Express, 2018,<br>5, 095203. | 1.6 | 24        |
| 221 | MyD88 is required for satellite cell-mediated myofiber regeneration in dystrophin-deficient mdx mice.<br>Human Molecular Genetics, 2018, 27, 3449-3463.   | 2.9 | 15        |
| 222 | TRAF3IP2 mediates TWEAK/TWEAKR-induced pro-fibrotic responses in cultured cardiac fibroblasts and the heart. Journal of Molecular and Cellular Cardiology, 2018, 121, 107-123.  | 1.9 | 26        |
| 223 | Critical points for electron–Mg atom elastic scattering. Journal of Physics B: Atomic, Molecular and<br>Optical Physics, 2018, 51, 035203.  | 1.5 | 6         |
| 224 | Electrically conductive MEH-PPV:PCL electrospun nanofibres for electrical stimulation of rat PC12 pheochromocytoma cells. Biomaterials Science, 2018, 6, 2342-2359.   | 5.4 | 29        |
| 225 | Synthesis of Yeast-Immobilized and Copper Nanoparticle-Dispersed Carbon Nanofiber-Based Diabetic<br>Wound Dressing Material: Simultaneous Control of Glucose and Bacterial Infections. ACS Applied Bio<br>Materials, 2018, 1, 246-258.                    | 4.6 | 52        |
| 226 | Oxygen-Releasing Antioxidant Cryogel Scaffolds with Sustained Oxygen Delivery for Tissue<br>Engineering Applications. ACS Applied Materials & Interfaces, 2018, 10, 18458-18469.  | 8.0 | 112       |
| 227 | Radiation interaction parameters of dosimetric importance for some commonly used compensators in IMRT using Monte Carlo simulation code. Journal of Radiological Protection, 2018, 38, 1321-1343.   | 1.1 | 0         |
| 228 | Effect of Mg2+ substitution on structural and magnetic properties of nano zinc ferrite. AIP<br>Conference Proceedings, 2018, , .  | 0.4 | 2         |
| 229 | Electrocatalytic Acitivity of rGO/PEDOT : PSS Nanocomposite towards Methanol Oxidation in Alkaline<br>Media. Electroanalysis, 2018, 30, 2131-2144.  | 2.9 | 15        |
| 230 | Effect of Annealing on Structural Properties of Fe3O4 Ferrite Nanoparticles. Advanced Science<br>Letters, 2018, 24, 5748-5751.  | 0.2 | 0         |
| 231 | Investigations on structural and magnetic properties of Mn doped Er 2 O 3. Solid State Sciences, 2017, 67, 8-12.  | 3.2 | 7         |
| 232 | Nano-Hydroxyapatite Bone Substitute Functionalized with Bone Active Molecules for Enhanced<br>Cranial Bone Regeneration. ACS Applied Materials & Interfaces, 2017, 9, 6816-6828.  | 8.0 | 91        |
| 233 | Up-Conversion in Perovskite Strontium Stannate Nanocrystal Whiskers. Transactions of the Indian<br>Institute of Metals, 2017, 70, 573-579.  | 1.5 | 9         |
| 234 | Constrained dipole oscillator strength distributions, sum rules, and dispersion coefficients for Br 2 and BrCN. Chemical Physics Letters, 2017, 672, 31-33.   | 2.6 | 1         |

| #   | Article   | IF   | CITATIONS |
|-----|---|------|-----------|
| 235 | Gamma ray shielding properties of PbO-Li 2 O-B 2 O 3 glasses. Radiation Physics and Chemistry, 2017, 136, 50-53.  | 2.8  | 206       |
| 236 | Design of quad-band microstrip-fed stubs-loaded frequency reconfigurable antenna for multiband operation. , 2017, , .   |      | 2         |
| 237 | Design and characterization of aperture coupled patch antenna for wearable applications. , 2017, , .  |      | 0         |
| 238 | A compact triple-band planar MIMO diversity antenna for WiMAX/WLAN applications. , 2017, , .  |      | 4         |
| 239 | Design of reconfigurable compact dual polarized antenna for multiband operation. , 2017, , .  |      | 3         |
| 240 | An extremely wideband/multiresonance monopole antenna with multiple notched stop bands. , 2017, , .   |      | 1         |
| 241 | Structural, optical and weak magnetic properties of Co and Mn codoped TiO 2 nanoparticles. Solid State Sciences, 2017, 73, 19-26.   | 3.2  | 32        |
| 242 | Design and analysis of a compact microstrip antenna using shorting pin for 5 GHz band. , 2017, , .  |      | 1         |
| 243 | A compact printed multistubs loaded resonator rectangular monopole antenna design for multiband wireless systems. International Journal of RF and Microwave Computer-Aided Engineering, 2017, 27, e21147. | 1.2  | 24        |
| 244 | MyD88 promotes myoblast fusion in a cell-autonomous manner. Nature Communications, 2017, 8, 1624.   | 12.8 | 46        |
| 245 | Impedance analysis and dielectric response of anatase TiO <sub>2</sub> nanoparticles codoped with<br>Mn and Co ions. Materials Research Express, 2017, 4, 115035.   | 1.6  | 6         |
| 246 | Effects of omega-3 on matrix metalloproteinase-9, myoblast transplantation and satellite cell activation in dystrophin-deficient muscle fibers. Cell and Tissue Research, 2017, 369, 591-602.             | 2.9  | 8         |
| 247 | A Four-Switch Single-Stage Single-Phase Buck–Boost Inverter. IEEE Transactions on Power<br>Electronics, 2017, 32, 5282-5292.  | 7.9  | 90        |
| 248 | A triple-band dual-polarized compact square slot antenna with an offset CPW feeding and radiator. ,<br>2017, , .  |      | 0         |
| 249 | A compact offset CPW-fed dual polarized stubs loaded monopole antenna for quad-band operation. , 2017, , .  |      | 3         |
| 250 | Compact offset CPW-fed inverted L-shaped dual-band dual-polarized reconfigurable printed antenna. ,<br>2017, , .  |      | 3         |
| 251 | High aperture efficiency profiled horn at Ku-band. , 2017, , .  |      | 1         |
| 252 | The PERK arm of the unfolded protein response regulates satellite cell-mediated skeletal muscle regeneration. ELife, 2017, 6, .   | 6.0  | 63        |

| #   | Article   | IF  | CITATIONS |
|-----|---|-----|-----------|
| 253 | A Compact ACS-Fed Triple-Band Dual-Polarized Stubs-Loaded Frequency Reconfigurable Printed Antenna for WiMAX and WLAN Applications. , 2017, , .   |     | 2         |
| 254 | Isolation, Culturing, and Differentiation of Primary Myoblasts from Skeletal Muscle of Adult Mice.<br>Bio-protocol, 2017, 7, .  | 0.4 | 60        |
| 255 | Distinct roles of TRAF6 and TAK1 in the regulation of adipocyte survival, thermogenesis program, and high-fat diet-induced obesity. Oncotarget, 2017, 8, 112565-112583.   | 1.8 | 16        |
| 256 | Pes Anserinus Bursitis due to Tibial Spurs in Children. Cureus, 2017, 9, e1427.   | 0.5 | 5         |
| 257 | EVALUATION OF DIAGNOSTIC PARAMETERS TO DETECT INDUCTION OF ACNE, ACUTE DERMAL IRRITATION<br>AND CORROSION POTENTIAL OF A POLYHERBAL FORMULATION. International Journal of Research in<br>Ayurveda and Pharmacy, 2017, 8, 87-90.   | 0.1 | 0         |
| 258 | Noncoding RNAs in the regulation of skeletal muscle biology in health and disease. Journal of<br>Molecular Medicine, 2016, 94, 853-866.   | 3.9 | 53        |
| 259 | A high voltage gain current fed non-isolated dc-dc converter. , 2016, , .   |     | 5         |
| 260 | Frequency domain analysis and design of isolated bidirectional series resonant Dc-dc converter. , 2016, , .   |     | 1         |
| 261 | Analysis and design of a current fed non-isolated buck-boost DC-DC converter. , 2016, , .   |     | 3         |
| 262 | Reconfigurable circular disc monopole UWB antenna with switchable two notched stop bands. , 2016, , .   |     | 8         |
| 263 | Dual band-notched circular disc monopole UWB antenna with switchable five notched stop bands. , 2016, , .   |     | 7         |
| 264 | A quad-band reconfigurable microstrip-fed circular disc monopole antenna for multiradio wireless systems. , 2016, , .   |     | 5         |
| 265 | Toll-like receptor signalling in regenerative myogenesis: friend and foe. Journal of Pathology, 2016, 239, 125-128.   | 4.5 | 24        |
| 266 | Constrained Dipole Oscillator Strength Distributions for CF <sub>4</sub> , CClF <sub>3</sub> ,<br>CCl <sub>2</sub> F <sub>2</sub> , CCl <sub>3</sub> F, CHF <sub>3</sub> , CH <sub>3</sub> F,<br>CH <sub>3</sub> Cl, CH <sub>3</sub> Br, CH <sub>3</sub> I, C <sub>2</sub> F <sub>6</sub> , and<br>CCl <sub>3</sub> CF <sub>3</sub> . Zeitschrift Fur Physikalische Chemie, 2016, 230, 1473-1486. | 2.8 | 2         |
| 267 | Studies on effective atomic numbers and electron densities of nucleobases in DNA. Radiation Physics and Chemistry, 2016, 127, 48-55.  | 2.8 | 21        |
| 268 | Dipole properties of PH3, PF3, PF5, PCl3, SiCl4, GeCl4, and SnCl4. Molecular Physics, 2016, 114, 1657-1663.   | 1.7 | 4         |
| 269 | Synthesis and Behavior of Cetyltrimethyl Ammonium Bromide Stabilized Zn1+xSnO3+x (0 ≤ â‰⊉)<br>Nano-Crystallites. PLoS ONE, 2016, 11, e0156246.  | 2.5 | 11        |
| 270 | Isolation, Culture, and Staining of Single Myofibers. Bio-protocol, 2016, 6, .  | 0.4 | 18        |

| #   | Article  | IF   | CITATIONS |
|-----|--|------|-----------|
| 271 | Morphology dependent catalytic activity of TiO2 nanostructures towards photodegradation of Rose<br>Bengal. AIP Conference Proceedings, 2015, , .   | 0.4  | 1         |
| 272 | Functional improvement after hip arthroscopy in cases of active paediatric hip joint tuberculosis: A<br>retrospective comparative study vis-Ã-vis conservative management. Journal of Children's<br>Orthopaedics, 2015, 9, 495-503.                                | 1.1  | 8         |
| 273 | Direct Repair without Augmentation of Patellar Tendon Avulsion following TKA. Case Reports in Orthopedics, 2015, 2015, 1-4.  | 0.3  | 4         |
| 274 | TAK1 modulates satellite stem cell homeostasis and skeletal muscle repair. Nature Communications, 2015, 6, 10123.  | 12.8 | 56        |
| 275 | Fe( <scp>iii</scp> ) induced structural, optical, and dielectric behavior of cetyltrimethyl ammonium<br>bromide stabilized strontium stannate nanoparticles synthesized by a facile wet chemistry route. RSC<br>Advances, 2015, 5, 17202-17209.                    | 3.6  | 33        |
| 276 | Elevated levels of TWEAK in skeletal muscle promote visceral obesity, insulin resistance, and metabolic dysfunction. FASEB Journal, 2015, 29, 988-1002.  | 0.5  | 21        |
| 277 | Structural and magnetic studies of the nickel doped CoFe2O4 ferrite nanoparticles synthesized by the chemical co-precipitation method. Journal of Magnetism and Magnetic Materials, 2015, 394, 379-384.  | 2.3  | 85        |
| 278 | Compact printed ultra-wideband antenna with two notched stop bands for WiMAX and WLAN.<br>International Journal of Applied Electromagnetics and Mechanics, 2015, 47, 523-531.  | 0.6  | 13        |
| 279 | Evaluation of pain in bilateral total knee replacement with and without tourniquet; aÂprospective randomized control trial. Journal of Clinical Orthopaedics and Trauma, 2015, 6, 85-88.   | 1.5  | 42        |
| 280 | Finite size effect on Sm3+ doped Mn0.5Zn0.5Sm Fe2â^'O4 (0â‰ <b>¤</b> â‰ <b>0</b> .5) ferrite nanoparticles. Ceramics<br>International, 2015, 41, 8623-8629.  | 4.8  | 36        |
| 281 | Effect of Gd3+ ion distribution on structural and magnetic properties in nano-sized Mn–Zn ferrite particles. Ceramics International, 2015, 41, 1297-1302.  | 4.8  | 35        |
| 282 | TRAF6 regulates satellite stem cell self-renewal and function during regenerative myogenesis. Journal of Clinical Investigation, 2015, 126, 151-168.   | 8.2  | 57        |
| 283 | Publication trend in the indian journal of orthopaedics: What is published and why?. Indian Journal of<br>Orthopaedics, 2015, 49, 661.   | 1.1  | 1         |
| 284 | COMPACT PLANAR MONOPOLE UWB ANTENNA WITH QUADRUPLE BAND-NOTCHED CHARACTERISTICS.<br>Progress in Electromagnetics Research C, 2014, 47, 29-36.  | 0.9  | 35        |
| 285 | Bizarre parosteal osteochondromatous proliferation (Nora's lesion) of phalanx in a child. BMJ Case<br>Reports, 2014, 2014, bcr2013201714-bcr2013201714.  | 0.5  | 9         |
| 286 | Design of an extremely wideband quasi-self-complementary pentagonal antenna with WLAN stop band. , 2014, , .   |      | 0         |
| 287 | DNA Methyltransferase 3a and Mitogen-activated Protein Kinase Signaling Regulate the Expression of<br>Fibroblast Growth Factor-inducible 14 (Fn14) during Denervation-induced Skeletal Muscle Atrophy.<br>Journal of Biological Chemistry, 2014, 289, 19985-19999. | 3.4  | 30        |
| 288 | A novel single stage, transformerless PV inverter. , 2014, , .   |      | 14        |

| #   | Article   | IF  | CITATIONS |
|-----|---|-----|-----------|
| 289 | A SEPIC derived single stage buck-boost inverter for photovoltaic applications. , 2014, , .   |     | 8         |
| 290 | Distinct roles of TRAF6 at early and late stages of muscle pathology in the mdx model of Duchenne muscular dystrophy. Human Molecular Genetics, 2014, 23, 1492-1505.  | 2.9 | 28        |
| 291 | TWEAK/Fn14 Signaling Axis Mediates Skeletal Muscle Atrophy and Metabolic Dysfunction. Frontiers in Immunology, 2014, 5, 18.   | 4.8 | 53        |
| 292 | Regulatory circuitry of TWEAKâ€Fn14 system and PGCâ€1α in skeletal muscle atrophy program. FASEB<br>Journal, 2014, 28, 1398-1411.   | 0.5 | 59        |
| 293 | Design and analysis of CPW-fed quasi-self-complementary pentagonal antenna for ultra-wideband systems. , 2014, , .  |     | 3         |
| 294 | An extremely wideband printed antenna with WLAN stop band using SRR. , 2014, , .  |     | 2         |
| 295 | The TWEAK–Fn14 dyad is involved in age-associated pathological changes in skeletal muscle.<br>Biochemical and Biophysical Research Communications, 2014, 446, 1219-1224.  | 2.1 | 29        |
| 296 | The TWEAK-Fn14 pathway: A potent regulator of skeletal muscle biology in health and disease. Cytokine and Growth Factor Reviews, 2014, 25, 215-225.   | 7.2 | 49        |
| 297 | Therapeutic potential of matrix metalloproteinases in Duchenne muscular dystrophy. Frontiers in<br>Cell and Developmental Biology, 2014, 2, 11.   | 3.7 | 47        |
| 298 | TWEAK promotes exercise intolerance by decreasing skeletal muscle oxidative phosphorylation capacity. Skeletal Muscle, 2013, 3, 18.   | 4.2 | 30        |
| 299 | Prevention of DoS Attacks in VANET. Wireless Personal Communications, 2013, 73, 95-126.   | 2.7 | 72        |
| 300 | Wasting mechanisms in muscular dystrophy. International Journal of Biochemistry and Cell Biology, 2013, 45, 2266-2279.  | 2.8 | 115       |
| 301 | Role of nonoperative treatment in managing degenerative tears of the medial meniscus posterior root. Journal of Orthopaedics and Traumatology, 2013, 14, 193-199.   | 2.3 | 62        |
| 302 | Proinflammatory Cytokine Tumor Necrosis Factor (TNF)-like Weak Inducer of Apoptosis (TWEAK)<br>Suppresses Satellite Cell Self-renewal through Inversely Modulating Notch and NF-I®B Signaling<br>Pathways. Journal of Biological Chemistry, 2013, 288, 35159-35169. | 3.4 | 36        |
| 303 | Signaling Mechanisms in Mammalian Myoblast Fusion. Science Signaling, 2013, 6, re2.   | 3.6 | 174       |
| 304 | Matrix Metalloproteinase-9 Inhibition Improves Proliferation and Engraftment of Myogenic Cells in Dystrophic Muscle of mdx Mice. PLoS ONE, 2013, 8, e72121.   | 2.5 | 65        |
| 305 | TWEAK and TRAF6 regulate skeletal muscle atrophy. Current Opinion in Clinical Nutrition and Metabolic Care, 2012, 15, 233-239.  | 2.5 | 85        |
| 306 | Analysis of Angelov model for 0.251̂¼m pHEMTs. Proceedings of SPIE, 2012, , .   | 0.8 | 0         |

| #   | Article  | IF  | CITATIONS |
|-----|--|-----|-----------|
| 307 | The E3 Ubiquitin Ligase TRAF6 Intercedes in Starvation-Induced Skeletal Muscle Atrophy through<br>Multiple Mechanisms. Molecular and Cellular Biology, 2012, 32, 1248-1259.            | 2.3 | 126       |
| 308 | Ultra-wideband truncated rectangular monopole antenna with band-notched characteristics. , 2012, , .   |     | 5         |
| 309 | Reciprocal Interaction between TRAF6 and Notch Signaling Regulates Adult Myofiber Regeneration upon Injury. Molecular and Cellular Biology, 2012, 32, 4833-4845.                       | 2.3 | 30        |
| 310 | Design, fabrication and measurement of sub 1 dB noise figure LNA. Proceedings of SPIE, 2012, , .   | 0.8 | 0         |
| 311 | TWEAK causes myotube atrophy through coordinated activation of ubiquitinâ€proteasome system, autophagy, and caspases. Journal of Cellular Physiology, 2012, 227, 1042-1051.            | 4.1 | 72        |
| 312 | Gene Profiling Studies in Skeletal Muscle by Quantitative Real-Time Polymerase Chain Reaction Assay.<br>Methods in Molecular Biology, 2012, 798, 311-324.                              | 0.9 | 9         |
| 313 | A compact ultra-wideband CPW-fed printed antenna with SRR for rejecting WLAN band. , 2011, , .   |     | 9         |
| 314 | Dipole polarizability, sum rules, mean excitation energies, and long-range dispersion coefficients for buckminsterfullerene C60. Chemical Physics Letters, 2011, 516, 208-211.         | 2.6 | 18        |
| 315 | Elevated levels of active matrix metalloproteinase-9 cause hypertrophy in skeletal muscle of normal and dystrophin-deficient mdx mice. Human Molecular Genetics, 2011, 20, 4345-4359.  | 2.9 | 63        |
| 316 | TRAF6 coordinates the activation of autophagy and ubiquitin-proteasome systems in atrophying skeletal muscle. Autophagy, 2011, 7, 555-556.   | 9.1 | 70        |
| 317 | Osteopontin-Stimulated Expression of Matrix Metalloproteinase-9 Causes Cardiomyopathy in the mdx<br>Model of Duchenne Muscular Dystrophy. Journal of Immunology, 2011, 187, 2723-2731. | 0.8 | 57        |
| 318 | Compact elliptical microstrip patch antenna with slotted ground for Ku-band applications. , 2011, , .  |     | 11        |
| 319 | Targeted ablation of TRAF6 inhibits skeletal muscle wasting in mice. Journal of Experimental Medicine, 2011, 208, i2-i2.   | 8.5 | 2         |
| 320 | Therapeutic targeting of signaling pathways in muscular dystrophy. Journal of Molecular Medicine, 2010, 88, 155-166.   | 3.9 | 40        |
| 321 | Do locking plates have a role in orthopaedic oncological reconstruction. Archives of Orthopaedic and Trauma Surgery, 2010, 130, 1493-1497.   | 2.4 | 9         |
| 322 | Tumor Necrosis Factor-α Regulates Distinct Molecular Pathways and Gene Networks in Cultured<br>Skeletal Muscle Cells. PLoS ONE, 2010, 5, e13262.                                       | 2.5 | 76        |
| 323 | Dlk1 Is Necessary for Proper Skeletal Muscle Development and Regeneration. PLoS ONE, 2010, 5, e15055.  | 2.5 | 108       |
| 324 | The TWEAK–Fn14 system is a critical regulator of denervation-induced skeletal muscle atrophy in mice.<br>Journal of Cell Biology, 2010, 188, 833-849.                                  | 5.2 | 205       |

| #   | Article  | IF  | CITATIONS |
|-----|--|-----|-----------|
| 325 | Transforming Growth Factor-β-activated Kinase 1 Is an Essential Regulator of Myogenic Differentiation.<br>Journal of Biological Chemistry, 2010, 285, 6401-6411.   | 3.4 | 38        |
| 326 | Targeted ablation of TRAF6 inhibits skeletal muscle wasting in mice. Journal of Cell Biology, 2010, 191, 1395-1411.  | 5.2 | 192       |
| 327 | Matrix Metalloproteinase Inhibitor Batimastat Alleviates Pathology and Improves Skeletal Muscle<br>Function in Dystrophin-Deficient mdx Mice. American Journal of Pathology, 2010, 177, 248-260.   | 3.8 | 71        |
| 328 | Genetic Ablation of TWEAK Augments Regeneration and Post-Injury Growth of Skeletal Muscle in Mice.<br>American Journal of Pathology, 2010, 177, 1732-1742.   | 3.8 | 53        |
| 329 | Genomic Profiling of Messenger RNAs and MicroRNAs Reveals Potential Mechanisms of TWEAK-Induced<br>Skeletal Muscle Wasting in Mice. PLoS ONE, 2010, 5, e8760.  | 2.5 | 73        |
| 330 | TNF-Like Weak Inducer of Apoptosis (TWEAK) Activates Proinflammatory Signaling Pathways and Gene<br>Expression through the Activation of TGF-Î <sup>2</sup> -Activated Kinase 1. Journal of Immunology, 2009, 182,<br>2439-2448.   | 0.8 | 62        |
| 331 | Tumor Necrosis Factor-related Weak Inducer of Apoptosis Augments Matrix Metalloproteinase 9<br>(MMP-9) Production in Skeletal Muscle through the Activation of Nuclear Factor-κB-inducing Kinase<br>and p38 Mitogen-activated Protein Kinase. Journal of Biological Chemistry, 2009, 284, 4439-4450. | 3.4 | 105       |
| 332 | Matrix metalloproteinase-9 inhibition ameliorates pathogenesis and improves skeletal muscle regeneration in muscular dystrophy. Human Molecular Genetics, 2009, 18, 2584-2598.   | 2.9 | 141       |
| 333 | Functional and radiological outcome after delayed fixation of femoral neck fractures in pediatric patients. Journal of Orthopaedics and Traumatology, 2009, 10, 211-216.   | 2.3 | 39        |
| 334 | Measurements of linear attenuation coefficients of irregular shaped samples by two media method.<br>Nuclear Instruments & Methods in Physics Research B, 2008, 266, 1116-1121.   | 1.4 | 8         |
| 335 | Protein–DNA array-based identification of transcription factor activities differentially regulated in skeletal muscle of normal and dystrophin-deficient mdx mice. Molecular and Cellular Biochemistry, 2008, 312, 17-24.  | 3.1 | 29        |
| 336 | Nuclear factor-kappa B signaling in skeletal muscle atrophy. Journal of Molecular Medicine, 2008, 86,<br>1113-1126.  | 3.9 | 338       |
| 337 | Effect of finite sample dimensions and total scatter acceptance angle on the gamma ray buildup factor. Annals of Nuclear Energy, 2008, 35, 2414-2416.  | 1.8 | 12        |
| 338 | Barium–borate–flyash glasses: As radiation shielding materials. Nuclear Instruments & Methods in<br>Physics Research B, 2008, 266, 140-146.  | 1.4 | 185       |
| 339 | ACCIDENTALLY FALLING INSTRUMENTS DURING ORTHOPAEDIC SURGERY: TIME TO WAKE UP!. ANZ Journal of Surgery, 2008, 78, 794-795.  | 0.7 | 13        |
| 340 | Kimura disease of extremity: Unusual manifestation in a long bone. Joint Bone Spine, 2008, 75, 492-494.  | 1.6 | 11        |
| 341 | Low grade central osteosarcoma – A diagnostic dilemma. Joint Bone Spine, 2008, 75, 613-615.  | 1.6 | 15        |
| 342 | Two Media Method: An Alternative Methodology for the Measurement of Attenuation Coefficients of<br>Irregularly Shaped Samples. Nuclear Science and Engineering, 2008, 159, 338-345.  | 1.1 | 0         |

| #   | Article  | IF  | CITATIONS |
|-----|--|-----|-----------|
| 343 | Regulation of Intracellular Signal Transduction Pathways by Mechanosensitive Ion Channels. , 2008, , 303-327.  |     | 4         |
| 344 | Tumor Necrosis Factor-α Augments Matrix Metalloproteinase-9 Production in Skeletal Muscle Cells<br>through the Activation of Transforming Growth Factor-β-activated Kinase 1 (TAK1)-dependent Signaling<br>Pathway. Journal of Biological Chemistry, 2007, 282, 35113-35124. | 3.4 | 53        |
| 345 | Transgenic Overexpression of Pregnancy-Associated Plasma Protein-A Increases the Somatic Growth and Skeletal Muscle Mass in Mice. Endocrinology, 2007, 148, 6176-6185.   | 2.8 | 33        |
| 346 | Assessing Drought Tolerance of Snap Bean (Phaseolus Vulgaris) From Genotypic Differences In Leaf<br>Water Relations,Shoot Growth and Photosynthetic Parameters. Plant Production Science, 2007, 10,<br>28-35.  | 2.0 | 25        |
| 347 | Influence Of Temperature Shift After Flowering on Dry Matter Partitioning In Two Cultivars of Snap<br>Bean (Phaseolus Vulgaris)That Differ In Heat Tolerance. Plant Production Science, 2007, 10, 14-19.   | 2.0 | 9         |
| 348 | TNFâ€related weak inducer of apoptosis (TWEAK) is a potent skeletal muscleâ€wasting cytokine. FASEB<br>Journal, 2007, 21, 1857-1869.   | 0.5 | 204       |
| 349 | To the Editor. Journal of Orthopaedic Trauma, 2007, 21, 670.   | 1.4 | 1         |
| 350 | An Improved Model for GaAs MESFETs Suitable for a Wide Bias Range. IEEE Microwave and Wireless<br>Components Letters, 2007, 17, 52-54.   | 3.2 | 4         |
| 351 | Fibroblast Growth Factor Inducible 14 (Fn14) Is Required for the Expression of Myogenic Regulatory<br>Factors and Differentiation of Myoblasts into Myotubes. Journal of Biological Chemistry, 2007, 282,<br>15000-15010.  | 3.4 | 76        |
| 352 | Studies on Effective Atomic Numbers and Electron Densities in Some Commonly Used Solvents.<br>Nuclear Science and Engineering, 2007, 155, 102-108.   | 1.1 | 8         |
| 353 | An unusual presentation of a rare chest wall tumour: Giant cell tumour of bone. Joint Bone Spine, 2007, 74, 100-102.   | 1.6 | 8         |
| 354 | A rare actinomycosis of humerus: an unusual location and a diagnostic dilemma. A case report.<br>Archives of Orthopaedic and Trauma Surgery, 2007, 128, 121-124.   | 2.4 | 3         |
| 355 | Influence of Irrigation Level, Growth Stages and Cultivars on Leaf Gas Exchange Characteristics in<br>Snap Bean (Phaseolus vulgaris) under Subtropical Environment. Japan Agricultural Research<br>Quarterly, 2007, 41, 201-206.   | 0.4 | 3         |
| 356 | Adaptation to Heat and Drought Stresses in Snap Bean (Phaseolus vulgaris) during the Reproductive<br>Stage of Development. Japan Agricultural Research Quarterly, 2006, 40, 213-216.   | 0.4 | 7         |
| 357 | Molar extinction coefficients of some commonly used solvents. Radiation Physics and Chemistry, 2006, 75, 737-740.  | 2.8 | 23        |
| 358 | Regulation of phosphatidylinositol 3-kinase (PI3K)/Akt and nuclear factor-kappa B signaling pathways in<br>dystrophin-deficient skeletal muscle in response to mechanical stretch. Journal of Cellular<br>Physiology, 2006, 208, 575-585.                                    | 4.1 | 92        |
| 359 | Influence of High Temperature on Morphological Characters, Biomass Allocation, and Yield<br>Components in Snap Bean (Phaseolus vulgarisL.). Plant Production Science, 2006, 9, 200-205.  | 2.0 | 11        |
| 360 | Tumor Necrosis Factor-like Weak Inducer of Apoptosis Inhibits Skeletal Myogenesis through Sustained<br>Activation of Nuclear Factor-κB and Degradation of MyoD Protein. Journal of Biological Chemistry,<br>2006, 281, 10327-10336.  | 3.4 | 139       |

| #   | Article  | IF  | CITATIONS |
|-----|--|-----|-----------|
| 361 | Variation of photon intensities in transmitted photon spectra of 60Co as a function of dimensions of a soil medium. Radiation Measurements, 2005, 39, 451-454.   | 1.4 | 2         |
| 362 | Inhibition of mechanosensitive cation channels inhibits myogenic differentiation by suppressing the expression of myogenic regulatory factors and caspaseâ€3 activity. FASEB Journal, 2005, 19, 1986-1997.   | 0.5 | 31        |
| 363 | Midday Drop of Leaf Water Content Related to Drought Tolerance in Snap Bean (Phaseolus vulgarisL.).<br>Plant Production Science, 2005, 8, 465-467.   | 2.0 | 29        |
| 364 | Pregnancy-associated Plasma Protein-A Regulates Myoblast Proliferation and Differentiation through<br>an Insulin-like Growth Factor-dependent Mechanism. Journal of Biological Chemistry, 2005, 280,<br>37782-37789.   | 3.4 | 42        |
| 365 | Reliable results for the Isotropic Dipole – Dipole and Triple – Dipole Dispersion Energy Coefficients<br>for Interactions involving Formaldehyde, Acetaldehyde, Acetone, and Mono - , Di - , and Tri -<br>Methylamine. Journal of Computational Methods in Sciences and Engineering, 2004, 4, 307-320.               | 0.2 | 3         |
| 366 | Loss of dystrophin causes aberrant mechanotransduction in skeletal muscle fibers. FASEB Journal, 2004, 18, 102-113.  | 0.5 | 141       |
| 367 | Cyclic mechanical strain inhibits skeletal myogenesis through activation of focal adhesion kinase,<br>Racâ€l GTPase, and NFâ€kB transcription factor. FASEB Journal, 2004, 18, 1524-1535.  | 0.5 | 105       |
| 368 | Nuclear factor-?B: its role in health and disease. Journal of Molecular Medicine, 2004, 82, 434-48.  | 3.9 | 834       |
| 369 | Energy and chemical composition dependence of mass attenuation coefficients of building materials.<br>Annals of Nuclear Energy, 2004, 31, 1199-1205.   | 1.8 | 75        |
| 370 | RF parameter extraction of MMIC nichrome resistors. Microwave and Optical Technology Letters, 2003, 39, 409-412.   | 1.4 | 15        |
| 371 | CCAAT/Enhancer-binding Protein and Activator Protein-1 Transcription Factors Regulate the<br>Expression of Interleukin-8 through the Mitogen-activated Protein Kinase Pathways in Response to<br>Mechanical Stretch of Human Airway Smooth Muscle Cells. Journal of Biological Chemistry, 2003, 278,<br>18868-18876. | 3.4 | 74        |
| 372 | Mechanical stretch activates nuclear factorâ€kappaB, activator proteinâ€1, and mitogenâ€activated protein<br>kinases in lung parenchyma: implications in asthma. FASEB Journal, 2003, 17, 1800-1811.   | 0.5 | 89        |
| 373 | Mechanical stress activates the nuclear factorâ€kappaB pathway in skeletal muscle fibers: a possible<br>role in Duchenne muscular dystrophy. FASEB Journal, 2003, 17, 386-396.   | 0.5 | 244       |
| 374 | Distinct Signaling Pathways Are Activated in Response to Mechanical Stress Applied Axially and<br>Transversely to Skeletal Muscle Fibers. Journal of Biological Chemistry, 2002, 277, 46493-46503.   | 3.4 | 84        |
| 375 | Human immunodeficiency virus-1-tat induces matrix metalloproteinase-9 in monocytes through protein tyrosine phosphatase-mediated activation of nuclear transcription factor NF-ήB. FEBS Letters, 1999, 462, 140-144.   | 2.8 | 53        |
| 376 | Assay for redox-sensitive kinases. Methods in Enzymology, 1999, 300, 339-345.  | 1.0 | 19        |
| 377 | Emodin (3-methyl-1,6,8-trihydroxyanthraquinone) inhibits TNF-induced NF-κB activation, IκB degradation,<br>and expression of cell surface adhesion proteins in human vascular endothelial cells. Oncogene, 1998,<br>17, 913-918.   | 5.9 | 160       |
| 378 | Corrosion inhibition of nickel in 4% nitric acid by substituted thione compounds. Materials Chemistry and Physics, 1998, 56, 243-248.  | 4.0 | 9         |

| #   | Article   | IF  | CITATIONS |
|-----|---|-----|-----------|
| 379 | Excitatory effects of muscarine on septohippocampal neurons: involvement of M3 receptors. Brain Research, 1998, 805, 220-233.   | 2.2 | 30        |
| 380 | Endotoxin-induced protein phosphorylation in macrophages is modulated by tumor cells.<br>International Journal of Immunopharmacology, 1998, 20, 99-110.   | 1.1 | 3         |
| 381 | Curcumin (Diferuloylmethane) Inhibition of Tumor Necrosis Factor (TNF)-Mediated Adhesion of<br>Monocytes to Endothelial Cells by Suppression of Cell Surface Expression of Adhesion Molecules and<br>of Nuclear Factor-IºB Activation. Biochemical Pharmacology, 1998, 55, 775-783. | 4.4 | 234       |
| 382 | Sanguinarine (Pseudochelerythrine) Is a Potent Inhibitor of NF-κB Activation, IκBα Phosphorylation, and<br>Degradation. Journal of Biological Chemistry, 1997, 272, 30129-30134.  | 3.4 | 257       |
| 383 | Effect of prolactin on nitric oxide and interleukin-1 production of murine peritoneal macrophages:<br>Role of Ca2+ and protein kinase C. International Journal of Immunopharmacology, 1997, 19, 129-133.  | 1.1 | 31        |
| 384 | On the anisotropy of the triple-dipole dispersion energy for interactions involving linear molecules.<br>Molecular Physics, 1996, 87, 845-858.  | 1.7 | 18        |
| 385 | Effect of Tumor Growth on the Blastogenic Response of Splenocytes: A Role of Macrophage-Derived<br>Nitric Oxide. Immunological Investigations, 1996, 25, 413-423.   | 2.0 | 27        |
| 386 | Gangliosides Produced by a T Cell Lymphoma Inhibit the Production of Reactive Nitrogen Intermediates by Murine Peritoneal Macrophages Journal of Clinical Biochemistry and Nutrition, 1996, 21, 171-182.  | 1.4 | 8         |
| 387 | Effect of cisplatin administration on the proliferation and differentiation of bone marrow cells of tumourâ€bearing mice. Immunology and Cell Biology, 1995, 73, 220-225.   | 2.3 | 13        |
| 388 | Effect of cisplatin and FK565 on the activation of tumor-associated and bone marrow-derived macrophages by Dalton's lymphoma. International Journal of Immunopharmacology, 1995, 17, 1-7.   | 1.1 | 21        |
| 389 | Giant congenital nevus. Indian Journal of Pediatrics, 1995, 62, 373-374.  | 0.8 | 0         |
| 390 | Effect of Dalton's lymphoma on the antigen presentation of murine peritoneal macrophages. Cancer<br>Letters, 1995, 92, 151-157.   | 7.2 | 13        |
| 391 | Valence shell absolute photoabsorption oscillator strengths, constrained dipole oscillator strength<br>distributions, and dipole properties for CH3NH2, (CH3)2NH, and (CH3)3N. Canadian Journal of<br>Chemistry, 1994, 72, 529-546.   | 1.1 | 21        |
| 392 | The absorption coefficient spectrum of poly(methyl methacrylate) in the soft X-ray region. Journal of<br>Polymer Science, Part B: Polymer Physics, 1992, 30, 185-195.   | 2.1 | 7         |
| 393 | A Synthetic Peptide, L-8-K, and Its Antibody Both Inhibit the Specific Binding of Vasoactive Intestinal<br>Peptide to Hamster Pancreatic Cancer Cells. Annals of the New York Academy of Sciences, 1988, 527,<br>679-681.   | 3.8 | 13        |
| 394 | Synthesis and biological activity of isodithiobiurets, dithiobiurets, and dithiazoles. Pharmaceutical Research, 1987, 04, 321-326.  | 3.5 | 14        |
| 395 | Total cross sections for positron scattering from argon atoms at intermediate energies. Physical Review A, 1986, 33, 2795-2797.   | 2.5 | 4         |
| 396 | Hindi-English "mixing" in scientific discourse. World Englishes, 1985, 4, 355-358.  | 1.1 | 1         |

| #   | Article  | IF  | CITATIONS |
|-----|--|-----|-----------|
| 397 | Differences in Osmoregulation in Brassica species. Annals of Botany, 1984, 54, 537-542.        | 2.9 | 49        |
| 398 | Elastic scattering of electrons by argon atoms. Pramana - Journal of Physics, 1978, 10, 63-73. | 1.8 | 12        |